

# Dalton Transactions

Accepted Manuscript



This is an *Accepted Manuscript*, which has been through the Royal Society of Chemistry peer review process and has been accepted for publication.

*Accepted Manuscripts* are published online shortly after acceptance, before technical editing, formatting and proof reading. Using this free service, authors can make their results available to the community, in citable form, before we publish the edited article. We will replace this *Accepted Manuscript* with the edited and formatted *Advance Article* as soon as it is available.

You can find more information about *Accepted Manuscripts* in the [Information for Authors](#).

Please note that technical editing may introduce minor changes to the text and/or graphics, which may alter content. The journal's standard [Terms & Conditions](#) and the [Ethical guidelines](#) still apply. In no event shall the Royal Society of Chemistry be held responsible for any errors or omissions in this *Accepted Manuscript* or any consequences arising from the use of any information it contains.

## ARTICLE

# Geometric and Electronic Structures of Five-Coordinate Manganese(II) “Picket Fence” Porphyrin Complexes

Cite this: DOI: 10.1039/x0xx00000x

Qiang Yu,<sup>a,b</sup> Yanhong Liu,<sup>c</sup> Diansheng Liu<sup>a</sup> and Jianfeng Li<sup>b,\*</sup>Received 00th January 2012,  
Accepted 00th January 2012

DOI: 10.1039/x0xx00000x

www.rsc.org/

Three five-coordinate, high spin manganese(II) “picket fence” porphyrin complexes, [Mn(TpivPP)(L)] (TpivPP = *a,a,a,a*-tetrakis(*o*-pivalamidophenyl)porphyrinato; L = 1-MeIm (1-methylimidazole), 1-EtIm (1-ethylimidazole) and 2-MeHIm (2-methylimidazole)) are synthesized and studied by single-crystal X-ray, UV-vis and electronic paramagnetic resonance (EPR) spectroscopies. Structural parameters are investigated and compared with analogues. Low temperature (90 K), high field EPR studies of [Mn(TpivPP)(1-MeIm)] and [Mn(TpivPP)(2-MeHIm)] observed five resonances including characteristic signals at ~5.9 and ~2.0. The simulations of the EPR spectra give the zero field splitting (zfs) parameters (*D*, *E* and  $\lambda$ ) and the hyperfine coupling constant (*A*).

## Introduction

A very important coordination group for heme proteins is the five-coordinate heme group with an axial histidine as the fifth ligand, often called the proximal histidine in the proteins.<sup>1</sup> Five-coordinate heme complexes play important roles in biochemical processes e.g. the cooperativity mechanism for oxygen binding, which is a transition between five-coordinate, high spin deoxyhemoglobin and six-coordinate, diamagnetic oxyhemoglobin.<sup>2</sup> Significant structural features in the transition include the movement of the iron atom with respect to the porphyrin plane, changes in axial bond length and porphyrin core conformation, and changes in orientation and off-axis tilts of the proximal histidine.<sup>3</sup> The extent and direction of the imidazole tilt can be very important, because they can dramatically change the steric interaction between the histidine and the porphyrin plane, essentially affecting the Fe—N<sub>His</sub> (histidine) bond strength.<sup>4</sup> As models of deoxyhemoglobin and deoxymyoglobin, imidazole-ligated five-coordinate iron(II) porphyrin analogues have been intensively studied.<sup>5,6,7</sup> A synthetic strategy for preparing five-coordinate imidazole ligated high-spin iron(II) derivatives used the sterically hindered 2-methylimidazole ligand.<sup>8</sup> A lot of progress has been made in this area, but difficulties exist, especially on the interpretations for electronic ground states.<sup>7,9</sup> Studies on ferric five-coordinate porphyrin complexes, [Fe(III)(Porph)(L)] (L = planar base ligand), is relatively small. The high spin

[Fe(OEP)(2-MeHIm)]<sup>+</sup> (OEP = 2,3,7,8,12,13,17,18-octaethylporphyrinato) had been the only structure of this class for many years since its report at 1985.<sup>10</sup> Recently Nakamura and coworkers reported highly *S*<sub>4</sub>-saddled [Fe(OETPP)(R-Im)]ClO<sub>4</sub> (OETPP = 2,3,7,8,12,13,17,18-octaethyl-*meso*-tetraphenylporphyrinato; R-Im = HIm (1H-imidazole), 2-MeHIm and 2-MeBzIm (2-methyl-benzimidazole)) which possess spin transition phenomena of iron.<sup>11</sup>

Research has indicated close similarities between the functional properties of hemoglobin and the manganese-substituted hemoglobins that display the same T → R conformational changes.<sup>12</sup> Manganese(II) is isoelectronic with iron(III) and the stereochemistry of high spin manganese(II) and high spin iron(III) porphyrins are expected to be dominated by the large size of the metal atom. This large size should yield derivatives in which the metal atom is substantially out of the porphyrin plane. Surprisingly, there is only one manganese(II) porphyrin complex [Mn(Porph)(L)] (L = planar base ligand) has been structurally characterized so far. [Mn(TPP)(1-MeIm)] (TPP = *meso*-tetraphenylporphyrinato), was reported by Scheidt and coworkers at 1977.<sup>13</sup> The authors suggested that manganese(II) derivatives have a distinct preference for five-coordination irrespective of the choice of axial ligand and when the *d*<sub>*x*<sup>2</sup>-*y*<sup>2</sup> orbital is populated, the metal atom is too far out of plane to permit effective interaction with a sixth (axial) ligand. In this work, three new, five-coordinate, high spin</sub>

manganese(II) “picket fence” porphyrin<sup>14</sup> complexes have been synthesized. We report the molecular structures and further examine the electronic configuration of these complexes.

## Experimental

### General Information

All experimental operations with Mn(II) complexes, including the reduction of Mn(III) were carried out using standard Schlenk ware and cannula techniques under argon unless otherwise noted. [H<sub>2</sub>(TpivPP)] (Figure S1) was prepared according to a local modification of the reported syntheses.<sup>14</sup> UV-vis spectra were recorded on a Perkin-Elmer Lambda-25 spectrometer, and FT-IR spectra were recorded on a Nicolet 6700 Fourier Transform Infrared Spectrometer as KBr pellets. Tetrahydrofuran (THF), benzene, hexanes (Sinopharm Chemical Reagent) were distilled from sodium and benzophenone, dichloromethane (CH<sub>2</sub>Cl<sub>2</sub>) and trichloromethane (CHCl<sub>3</sub>) were distilled from CaH<sub>2</sub> (Greagent), ethyl alcohol (EtOH) (Sinopharm Chemical Reagent) was distilled from magnesium rod (Sinopharm Chemical Reagent), pivaloyl chloride, ethanethiol, 2,6-lutidine (Aladdin Industrial Inc.), 1-MeIm (ACROS) and 1-EtIm were distilled in an Ar atmosphere and 2-MeHIm was recrystallized from benzene before use. MnCl<sub>2</sub> (Aladdin Industrial Inc., AR, 99.0%) was used without further purification.

**Synthesis of [Mn(TpivPP)Cl].** H<sub>2</sub>TpivPP (2 g, 1.98 mmol), 2,6-lutidine (1 mL) and anhydrous MnCl<sub>2</sub> (3.71 g, 29.69 mmol) in THF (200 mL) were heated to reflux under argon. The reaction was finished in 6 hours. The mixture was brought to dryness on a rotary evaporator and extracted with CH<sub>2</sub>Cl<sub>2</sub>. The filtrate was treated with diluted HCl solution and then washed with distilled water three times, dried over anhydrous magnesium sulfate, filtered and evaporated to dryness. The resulting solid was chromatographed on a column of silica gel (benzene: diethyl ether; 2.5: 1). The first fraction was collected to give 1.4 g product (65%). UV-vis (CHCl<sub>3</sub>): 368, 476, 530, 580, 614 nm.

**Synthesis of [Mn(TpivPP)]<sub>2</sub>O.** A CH<sub>2</sub>Cl<sub>2</sub> (25 mL) solution of [Mn(TpivPP)Cl] (0.5 g) was treated vigorously with 3M KOH solution three times, and dried over anhydrous magnesium sulfate. After filtration, the filtrate was brought to dryness on a rotary evaporator. The resulting solid was chromatographed on a column of silica gel, eluted with benzene: diethyl ether (2.5: 1) and then methanol. The last fraction was collected to give 0.3 g product (62%). UV-vis (benzene): 371, 398, 420, 473, 577, 610 nm. FT-IR  $\nu$  (Mn—O): 833 cm<sup>-1</sup>.

**Synthesis of [Mn(TpivPP)].** [Mn(TpivPP)]<sub>2</sub>O (40 mg, 18.66 × 10<sup>-3</sup> mmol) was dried in vacuum for 30 min and dissolved in 5 mL benzene. 2 mL ethanethiol was added to the solution. The solution was stirred for 2 days and evacuated in vacuum to give dark purple powder. UV-vis (THF): 435, 527, 565, 610 nm.

**Synthesis of [Mn(TpivPP)(1-MeIm)].** The purple solid of [Mn(TpivPP)] (10 mg, 9.33 × 10<sup>-3</sup> mmol) was dried in vacuum

for 30 min and dissolved in 2.5 mL THF. 0.04 mL (0.5 mmol) of 1-methylimidazole was added. The mixture was stirred for 20 min and transferred into glass tubes (8 mm × 10 cm) which were layered with hexanes as nonsolvent. Several days later, X-ray quality, block crystals were collected. UV-vis (THF): 442, 532, 573, 611 nm.

**Synthesis of [Mn(TpivPP)(1-EtIm)].** Similar reaction procedures as above were performed. Several days later, block crystalline product was collected. UV-vis (THF): 444, 535, 574, 614 nm.

**Synthesis of [Mn(TpivPP)(2-MeHIm)].** The purple solid [Mn(TpivPP)] (10 mg, 9.33 × 10<sup>-3</sup> mmol) was dried in vacuum for 30 min and dissolved in 2.5 mL benzene. To this solution 3.8 mg 2-methylimidazole (4.67 × 10<sup>-2</sup> mmol) and 8 drops of ethanol were added. The mixture was stirred for 20 min and transferred into glass tubes (8 mm × 10 cm) which were layered with hexanes as nonsolvent. Several days later, block crystals were collected. UV-vis (THF): 444, 535, 573, 613 nm.

### X-ray Structure Determinations

Single-crystal experiment of [Mn(TpivPP)(1-EtIm)] was carried out on a Bruker Apex system with graphite-monochromated Mo K $\alpha$  radiation ( $\lambda = 0.71073$  Å). Single-crystal experiments of [Mn(TpivPP)(1-MeIm)] and [Mn(TpivPP)(2-MeHIm)] were carried out on a Xcalibur, Eos, Gemini system with graphite-monochromated Mo K $\alpha$  radiation ( $\lambda = 0.71073$  Å). The crystalline samples were placed in inert oil, mounted on a glass pin, transferred to the cold gas stream of the diffractometer, and crystal data collected at 121 or 150 K. The structures were solved by direct methods (SHELXS-97) and refined against  $F^2$  using SHELXL-97.<sup>15,16</sup> Subsequent difference Fourier syntheses led to the location of all remaining non-hydrogen atoms. For the structure refinement, all data were used including negative intensities. All non-hydrogen atoms were refined anisotropically if not remarked upon otherwise below. Hydrogen atoms were idealized with the standard SHELXL-97 idealization methods. The program SADABS<sup>17</sup> was applied for the absorption correction of [Mn(TpivPP)(1-EtIm)] structure. The data sets of [Mn(TpivPP)(1-MeIm)] and [Mn(TpivPP)(2-MeHIm)] were corrected by empirical absorption correction using spherical harmonics, implemented in the SCALE3 ABSPACK scaling algorithm.<sup>18</sup>

**[Mn(TpivPP)(1-MeIm)]·THF.** A black crystal with the dimensions 0.35 × 0.25 × 0.20 mm<sup>3</sup> was used for the structure determination. In this structure, the asymmetric unit contains a half picket fence porphyrin and THF solvent molecules. There is a crystallographic 2-fold axis passing through the manganese atom. The 1-MeIm ligand and the THF molecule were found to disorder between 2-fold symmetry related sites. The six atoms of imidazole were restrained by “similar U<sub>ij</sub>” (SIMU) to constrain the anisotropic displacement parameters (ADP). The ordered THF molecule was refined isotropically.

**[Mn(TpivPP)(1-EtIm)]·CH<sub>2</sub>Cl<sub>2</sub>.** A black crystal with the dimensions 0.10 × 0.20 × 0.20 mm<sup>3</sup> was used for the structure determination. The asymmetric unit contains one five-coordinate picket fence porphyrin complex and one

dichloromethane solvent molecule. The 1-EtIm ligand was found to disorder over two positions and the site occupancy factors (SOFs) of disordered moieties are refined by means of “free variable”. The final SOFs are found to be 0.66 and 0.34. Three carbon atoms (C41, C42 and C43) on one of the four *tert*-butyl groups and three atoms (N9A, N10A and C49A) on the imidazole exhibited unusual thermal motions, thus the six atoms were restrained by “ISOR” commands. The five atoms (C46, C49A, C49B, N9A and N10A) of imidazole were restrained by “similar  $U_{ij}$ ” (SIMU) to constrain the ADP.

**[Mn(TpivPP)(2-MeHIm)]·0.2EtOH.** A black crystal with the dimensions  $0.25 \times 0.20 \times 0.20$  mm<sup>3</sup> was used for the structure determination. In this structure, the asymmetric unit contains one half picket fence porphyrin and a disordered ethanol solvent molecule. There is a crystallographic 2-fold axis passing through the manganese atom. The 2-MeHIm ligand and ethanol molecule were found to disorder between 2-fold related sites. Two carbon atoms (C23 and C24) on the imidazole ring were restrained by “similar  $U_{ij}$ ” (SIMU) to constrain the ADP. The N and O atoms on one of the four amide groups were disordered over two positions. The O2 and O1A atoms on the carbonyl groups and C15 atom on one of the four pickets was exhibited unusual thermal motions, thus restrained by “ISOR” commands. The ethanol molecule possesses a 2-fold axis with C2S and O1S on the axis, C1S, C2S and O1S were restrained by “similar  $U_{ij}$ ” (SIMU) to constrain the ADP and by “ISOR” commands.

## EPR

X-band continuous wave (cw) electron paramagnetic resonance (EPR) measurements were carried out on a Bruker E500 EPR spectrometer at a microwave frequency of 9.45 GHz using a liquid nitrogen cooling system. The EPR spectra were measured at 90 K with a modulation amplitude of 0.3 mT, a modulation frequency of 100 kHz and a microwave power of 10.02 mW. EPR spectra of [Mn(TpivPP)(1-MeIm)] were recorded on microcrystalline powder obtained by carefully adding an excess of hexanes to the THF solution of [Mn(TpivPP)(1-MeIm)]. EPR spectra of [Mn(TpivPP)(2-MeHIm)] were recorded on solid and solution states. The microcrystalline powder sample was obtained by grinding a sufficient quantity of crystals; the solution sample was made by dissolving the microcrystalline powder in methylene chloride solvent. The EPR spectra were simulated with the EasySpin package.<sup>19</sup>

## Results

The synthesis, UV-vis spectra, molecular structures and EPR spectra of three new five-coordinate, manganese picket fence porphyrinates, [Mn(TpivPP)(1-MeIm)], [Mn(TpivPP)(1-EtIm)] and [Mn(TpivPP)(2-MeHIm)] are reported. The UV-vis spectra of [Mn(TpivPP)(1-MeIm)], [Mn(TpivPP)(1-EtIm)] and [Mn(TpivPP)(2-MeHIm)] are given in Figures S2–S4 of Electronic Supplementary Information (ESI). The spectrum of [Mn(TpivPP)(1-MeIm)] exhibits the Soret band maximum at

442 and Q bands at 532, 573, 611 nm (Figure S2), which are consistent with that of [Mn(TPP)(1-MeIm)] and [Mn(TPP)(2-MeHIm)].<sup>20</sup> [Mn(TpivPP)(1-EtIm)] and [Mn(TpivPP)(2-MeHIm)] show very similar spectra with Soret bands at 444 nm (Figures S3 and S4).

The labeled Oak Ridge thermal ellipsoid plot (ORTEP) of three picket fence porphyrinates is given in Figures 1, 2 and 3. A brief summary of the crystallographic data is given in Table 1, and the complete crystallographic details, atomic coordinates, bond distances, bond angles of these three structures are given in Crystallographic Information File (CIF).

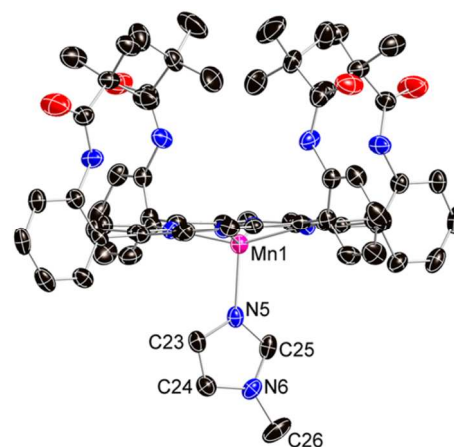
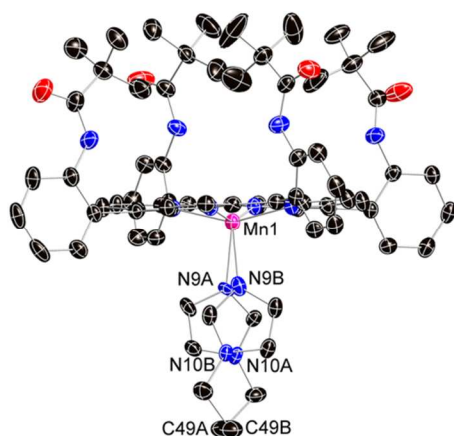


Figure 1. Thermal ellipsoid plot of [Mn(TpivPP)(1-MeIm)] displaying a partial atom labeling scheme. The molecule has a required 2-fold axis of symmetry perpendicular to the porphyrin plane. Thus the axial imidazole is disordered over two positions related by the required symmetry axis, but only one orientation is shown. Thermal ellipsoids of all atoms are contoured at the 40% probability level. Hydrogen atoms molecule have been omitted for clarity.

Additional quantitative information of the three structures is given in Figure 4, which displays the detailed displacements of each porphyrin core atom (in units of 0.01 Å) from the 24-atom mean planes. The orientation of the imidazole ligands including the value of the dihedral angles are also given; the circle represents the position of the methyl (or ethyl) groups on each ligand. The top panel of Figure 4 shows the porphyrin core of [Mn(TpivPP)(1-MeIm)] which has a near-planar porphyrin conformation. The displacements of *meso* and  $\beta$  carbon atoms are  $\leq 0.14$  Å. The mean Mn—N<sub>p</sub> (porphyrinato nitrogen) bond length is 2.1285(6) Å. The out-of-plane displacement of the metal center relative to the 24-atom mean plane ( $\Delta_{24}$ ) is 0.56 Å. The asymmetric unit of the [Mn(TpivPP)(1-EtIm)] contains one full porphyrin molecule, which is different from the other two structures where half porphyrin moieties are found in the asymmetric units because of the crystallographic required symmetry. As seen in the middle panel of Figure 4, the porphyrin core is also near-planar. The mean Mn—N<sub>p</sub> bond distance is 2.122(3) Å. The manganese center lies out of the mean plane of the 24 core atoms with  $\Delta_{24} = 0.54$  Å. The disordered imidazole ligand causes two different Mn—N<sub>Im</sub> (nitrogen of imidazole) bond distances and dihedral angles to the closest N<sub>p</sub>—Mn—N<sub>Im</sub> planes. As seen in the bottom panel of Figure 4, the porphyrin core of [Mn(TpivPP)(2-MeHIm)]

also shows a near-planar conformation. The average Mn—N<sub>p</sub> bond distance is 2.129(3) Å. The manganese atom has the largest out of plane displacement among these three structures ( $\Delta_{24} = 0.60$  Å). The dihedral angle between 2-MeHIm plane and the plane of the closest N<sub>p</sub>—Mn—N<sub>Im</sub> is 28.1°.



**Figure 2.** Thermal ellipsoid plot of [Mn(TpivPP)(1-EtIm)] displaying a partial atom labeling scheme. The axial imidazole is disordered over two positions. Thermal ellipsoids of all atoms are contoured at the 40% probability level. Hydrogen atoms have been omitted for clarity.

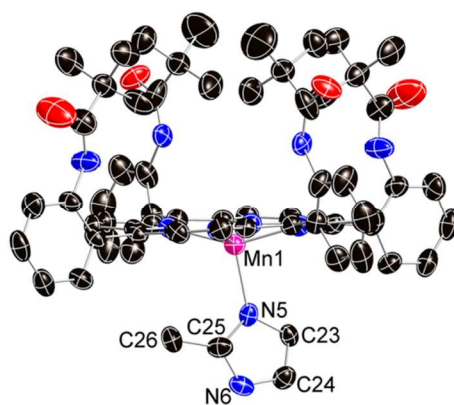


**Figure 3.** Thermal ellipsoid plot of [Mn(TpivPP)(2-MeHIm)] displaying a partial atom labeling scheme. The molecule has a required 2-fold axis of symmetry perpendicular to the porphyrin plane. Thus the axial imidazole is disordered over two positions related by the required symmetry axis, but only one orientation is shown. Thermal ellipsoids of all atoms are contoured at the 40% probability level. Hydrogen atoms have been omitted for clarity.

## Discussion

### Structures

Thermal ellipsoid diagrams of [Mn(TpivPP)(1-MeIm)], [Mn(TpivPP)(1-EtIm)] and [Mn(TpivPP)(2-MeHIm)] are presented in Figures 1, 2 and 3, which shows the view parallel to the porphyrin plane. The top-down thermal ellipsoid diagrams of the three complexes are given in Figures S5–S7 of ESI. It is seen that three porphyrin complexes share some common features. All imidazole ligands are outside the molecular cavities on the unhindered porphyrin side. All axial ligands are disordered over two positions. In the structures of [Mn(TpivPP)(1-MeIm)] and [Mn(TpivPP)(2-MeHIm)] (both in

space group of *C2/c*, with required 2-fold symmetry), the two imidazole ligands are disordered between two 2-fold related sites, but only one position is shown in Figures 1 and 3. In the structure of [Mn(TpivPP)(1-EtIm)] (space group of *P2<sub>1</sub>/c*), the 1-EtIm is disordered over two crystallographic independent positions and both orientational parts are shown in Figure 2. All three porphyrin planes are near planar. The high spin Mn(II) atom is significantly displaced out of the porphyrin plane, which induces noticeable porphyrin core doming and long Mn—N<sub>p</sub> bonds. All four protecting *tert*-butyl pickets of the three derivatives are ordered, similar to the five-coordinate analogues of [M(TpivPP)(2-MeHIm)] (M = Co and Fe).<sup>6,21,22</sup>

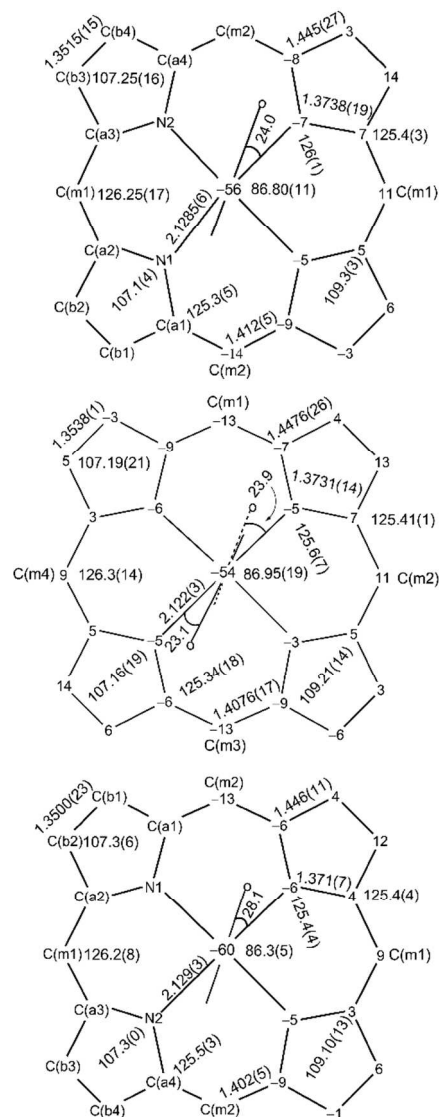


**Figure 4.** Formal diagrams of the porphyrinato cores of [Mn(TpivPP)(1-MeIm)] (top), [Mn(TpivPP)(1-EtIm)] (middle) and [Mn(TpivPP)(2-MeHIm)] (bottom). Averaged values of the chemically unique bond distances (in Å) and angles (in degrees) are shown. The numbers in parentheses are the esd's calculated on the assumption that the averaged values were all drawn from the same population. The perpendicular displacements (in units of 0.01 Å) of the porphyrin core atoms from the 24-atom mean plane are also displayed. In all diagrams, positive values of the displacement are towards the hindered porphyrin side, the solid line and dashed line indicate the plane of imidazole on the unhindered porphyrin side.

**Table 1.** Complete Crystallographic Details for [Mn(TpivPP)(1-MeIm)]·THF, [Mn(TpivPP)(1-EtIm)]·CH<sub>2</sub>Cl<sub>2</sub> and [Mn(TpivPP)(2-MeHIm)]·0.2EtOH

	[Mn(TpivPP)(1-MeIm)]·THF	[Mn(TpivPP)(1-EtIm)]·CH <sub>2</sub> Cl <sub>2</sub>	[Mn(TpivPP)(2-MeHIm)]·0.2EtOH
chemical formula	C <sub>72</sub> H <sub>78</sub> MnN <sub>10</sub> O <sub>5</sub>	C <sub>70</sub> H <sub>74</sub> Cl <sub>2</sub> MnN <sub>10</sub> O <sub>4</sub>	C <sub>68.4</sub> H <sub>71.2</sub> MnN <sub>10</sub> O <sub>4.2</sub>
FW	1218.38	1245.23	1155.49
<i>a</i> , Å	18.5236(6)	18.5198(7)	18.5139(5)
<i>b</i> , Å	19.3393(6)	19.3485(6)	19.1542(5)
<i>c</i> , Å	18.2222(4)	18.1151(7)	18.2771(4)
<i>β</i> , deg	90.283(2)	90.5590(1)	90.646(2)
<i>V</i> , Å <sup>3</sup>	6528.7(3)	6490.9(4)	6481.0(3)
space group	<i>C2/c</i>	<i>P2<sub>1</sub>/c</i>	<i>C2/c</i>
<i>Z</i>	4	4	4
cryst dimensions (mm)	0.20 × 0.25 × 0.35	0.10 × 0.20 × 0.20	0.20 × 0.20 × 0.25
temp, K	150(2)	150(2)	121(2)
total data collected	23493	135851	32608
unique data	5735 ( <i>R</i> <sub>int</sub> = 0.045)	13283 ( <i>R</i> <sub>int</sub> = 0.061)	5694 ( <i>R</i> <sub>int</sub> = 0.070)
unique obsd data	4251	10174	3969
[ <i>I</i> > 2σ( <i>I</i> )]			
GOF (based on <i>F</i> <sup>2</sup> )	1.037	1.054	1.053
<i>D</i> <sub>calcd</sub> , g cm <sup>-3</sup>	1.240	1.274	1.184
<i>μ</i> , mm <sup>-1</sup>	0.261	0.342	0.258
final <i>R</i> indices	<i>R</i> <sub>1</sub> = 0.0519	<i>R</i> <sub>1</sub> = 0.0559	<i>R</i> <sub>1</sub> = 0.0954
[ <i>I</i> > 2σ( <i>I</i> )]	<i>wR</i> <sub>2</sub> = 0.1255	<i>wR</i> <sub>2</sub> = 0.1416	<i>wR</i> <sub>2</sub> = 0.2758
final <i>R</i> indices	<i>R</i> <sub>1</sub> = 0.0765	<i>R</i> <sub>1</sub> = 0.0796	<i>R</i> <sub>1</sub> = 0.1249
(all data)	<i>wR</i> <sub>2</sub> = 0.1382	<i>wR</i> <sub>2</sub> = 0.1633	<i>wR</i> <sub>2</sub> = 0.3081

It is interesting to note that the pickets of all known five-coordinate picket fence porphyrinates are ordered, when the axial ligand is located on the unhindered porphyrin side. However for the six-coordinate picket fence porphyrinates with small molecules in the cavities, disordered pickets are usually observed. In the studies of oxy-iron and -cobalt picket fence porphyrinates [M(TpivPP)(R-Im)(O<sub>2</sub>)] (M = Fe, Co; R-Im = 1-MeIm, 1-EtIm and 2-MeHIm), multi-temperature single crystal characterization has revealed the correlated oxygen and pickets motions that lead to the mutual ligand disorder.<sup>22,23</sup>

The manganese(II) porphyrinates prefer to form five-coordinate high spin complexes. This appears to result from the inability of axial ligands to effect a change from a high spin to a low spin manganese(II) configuration. The metal atom is too far out of the porphyrin plane to permit effective interaction with a sixth ligand.<sup>13</sup> This is compared to the cobalt(II) porphyrinates where only five-coordinate low spin derivatives result from the reaction of four-coordinate cobalt(II) porphyrin with any imidazole derivatives.<sup>21</sup> The difficulty of forming a six-coordinate species from a five-coordinate low spin [Co(Porph)(R-Im)] may be understood in terms of the destabilization of *d*<sub>z<sup>2</sup></sub> orbital.<sup>24</sup>

The key parameters of all four structurally characterized

[Mn(II)(Porph)(L)] are given in Table 2. Also given are the structural parameters of picket fence analogues of [Fe(TpivPP)(2-MeHIm)],<sup>22</sup> [Co(TpivPP)(2-MeHIm)]<sup>21</sup> and [Fe(OEP)(2-MeHIm)]<sup>+</sup> which is the only five-coordinate iron(III) porphyrin structure with a near planar porphyrin plane.<sup>10</sup>

The overall structural features of the manganese species are those expected for a high-spin Mn(II) complex.<sup>5b</sup> These include an expanded porphyrin core, stretched equatorial Mn—N<sub>p</sub> bonds, and a significant out-of-plane displacement of the Mn(II) atom. The metal atom displacements from the 24-atom mean plane ( $\Delta_{24}$ ) and the four nitrogen atoms plane ( $\Delta_4$ ) are seen to be different and sometimes significantly different for any given derivative. The difference in the two values (note that  $\Delta_{24}$  is always larger than  $\Delta_4$ ) is a measure of porphyrin core doming. Porphyrin core doming is observed for metalloporphyrin derivatives with metal ions that are too large to fit into the central hole of the porphyrin ring.<sup>25</sup> It is seen that manganese(II) complexes show the largest  $\Delta_{24}$  and  $\Delta_4$  among the three metalloporphyrin sets. The high spin (HS) Fe(II) displaced slightly more than the HS Fe(III), and the low spin (LS) Co(II) atom shows the smallest displacement. Thus the metal out-of-plane displacements have the following sequence: HS Mn(II) >

Table 2. Selected Structural Parameters for Five-Coordinate [M(TpivPP)(L)] and related species.<sup>a</sup>

complex	(M—N <sub>p</sub> ) <sub>av</sub> <sup>b</sup>	M—N <sub>im</sub>	Δ <sub>4</sub> <sup>c</sup>	Δ <sub>24</sub> <sup>d</sup>	M—N <sub>im</sub> —C <sub>im</sub> (2) <sup>e</sup>	M—N <sub>im</sub> —C <sub>im</sub> (4) <sup>f</sup>	φ <sup>g</sup>	τ <sup>h</sup>	ref.
Mn(II) Complexes									
[Mn(TpivPP)(1-MeIm)]	2.1285(6)	2.168(5)	0.50	0.56	128.8(9)	125.5(8)	24.0	5.2	tw
[Mn(TpivPP)(1-EtIm)]	2.122(3)	2.216(19)	0.49	0.54	131.4(9)	120.5(11)	23.1	6.8	tw
		2.120(13)			129.5(6)	125.6(5)	23.9	4.1	
[Mn(TpivPP)(2-MeHIm)]	2.129(3)	2.177(9)	0.54	0.60	126.4(7)	128.1(9)	28.1	9.8	tw
[Mn(TPP)(1-MeIm)]	2.128(7)	2.192(2)	0.51	0.56	130.4(2)	125.2(2)	15.4	10.9	13
Fe(II, III) Complexes									
[Fe(TpivPP)(2-MeHIm)]	2.070(6)	2.113(3)	0.35	0.38	128.5(2)	125.7(3)	23.3	8.3	22
[Fe(OEP)(2-MeHIm)] <sup>+</sup>	2.038(6)	2.068(4)	0.35	0.36	131.7(3)	122.1(3)	4.0	5.0	10
Co(II) Complex									
[Co(TpivPP)(2-MeHIm)]	1.979(3)	2.145(3)	0.14	0.15	132.0(3)	123.1(3)	21.6	6.5	21

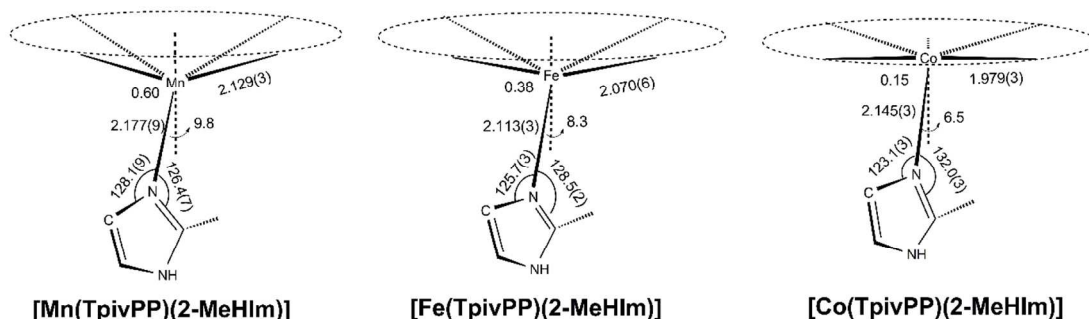
<sup>a</sup> Estimated standard deviations are given in parentheses; Distances in Å, angles in degree. <sup>b</sup> Averaged value. <sup>c</sup> Displacement of metal atom from the four pyrrole N atoms mean plane. <sup>d</sup> Displacement of metal atom from the 24-atom mean plane. <sup>e</sup> M—N<sub>im</sub>—C<sub>im</sub> angle with C<sub>im</sub> being the 2-carbon of imidazole ring, sometimes methyl substituted. <sup>f</sup> M—N<sub>im</sub>—C<sub>im</sub> angle with C<sub>im</sub> being the 4-carbon of imidazole ring. <sup>g</sup> Dihedral angle between the plane of the closest N<sub>p</sub>—M—N<sub>im</sub> and the ligand plane. <sup>h</sup> Off-axis tilt of the M—N<sub>im</sub> vector from the normal to the core.

HS Fe(II) > HS Fe(III) > LS Co(II), which follow the metal ion radius.<sup>26</sup> Larger metal displacements give longer M—N<sub>p</sub> bond distances. It is seen in Table 2 that the lengths of (M—N<sub>p</sub>)<sub>av</sub> (averaged value) bonds are consistent with the metal out of plane displacements. Manganese complexes with its largest metal displacements give the longest (M—N<sub>p</sub>)<sub>av</sub> bond distances, while the low spin cobalt complex has the smallest metal displacement and the shortest (M—N<sub>p</sub>)<sub>av</sub> bond distance.

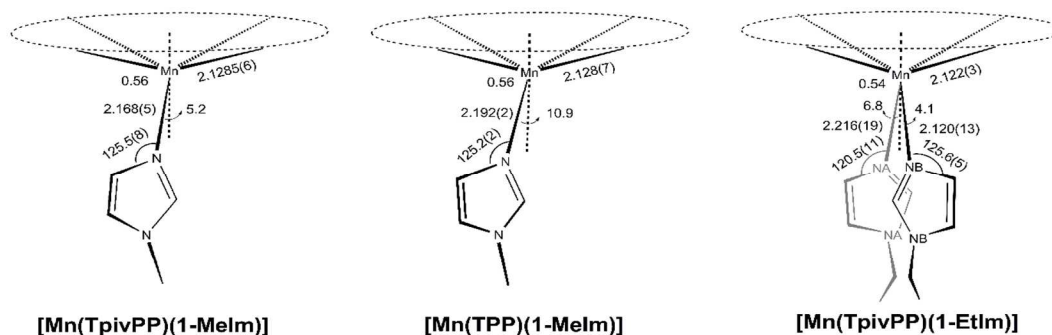
There are several necessary structural responses to binding a hindered imidazole to form five-coordinate porphyrinates. The overall effect required is to maximize the attractive interaction between metal and its ligands while minimizing the repulsive interaction between the 2-methyl group of the imidazole ligand and the porphyrin plane. This can be accomplished by (geometric) adjustments of the porphyrin plane and the hindered imidazole. The imidazole adjustments include the tilting of the M—N<sub>im</sub> bond off the normal to the porphyrin plane (conventionally denoted τ angles), a rotation of the imidazole ligand that leads to unequal M—N<sub>im</sub>—C<sub>im</sub> (carbon of imidazole ring) angles, the M—N<sub>im</sub> bond length and the orientation of imidazole plane with respect to the porphyrin core. Several structural features of [Mn(TpivPP)(2-MeHIm)] suggest that the 2-MeHIm is not strongly sterically stressed. The porphyrin plane of [Mn(TpivPP)(2-MeHIm)] is fairly planar, at the same level of the unhindered imidazole derivatives as seen in Figure 4. The Mn—N<sub>im</sub>—C<sub>im</sub>(2) angle on the 2-methyl group side is smaller than the Mn—N<sub>im</sub>—C<sub>im</sub>(4) angle on the 4-position side, which is in sharp contrast to the corresponding angles in [M(TpivPP)(2-MeHIm)] (M = Fe, Co) analogues. The key parameters of these three five-coordinate picket fence porphyrin analogues [M(TpivPP)(2-MeHIm)] (M = Mn, Fe, Co) are given in Scheme 1 for comparison. It is seen that in the iron and cobalt structures, the

angles of M—N<sub>im</sub>—C<sub>im</sub>(2) are larger than M—N<sub>im</sub>—C<sub>im</sub>(4) and the difference between the two unequal angles are correlated to the metal out of plane displacements. The smaller metal displacement of cobalt atom (0.15 vs. 0.38 Å) corresponds to larger angle difference (8.9 vs. 2.8°), which suggests that the unequal angles are a result of imidazole rotation because of the steric 2-methyl group and the smaller metal displacement induces more 2-MeHIm ligand rotation to maximize the distance between the 2-methyl group and porphyrin core atoms. Hence, the structure of [Mn(TpivPP)(2-MeHIm)] presents a very different case by showing a smaller Mn—N<sub>im</sub>—C<sub>im</sub>(2) angle on the 2-methyl group side, which indicates that the 2-methyl imidazole is not strongly sterically stressed.

We now consider the [Mn(II)(Porph)(L)] structures with unhindered imidazole ligands. Scheme 2 depicts the key parameters of three [Mn(II)(Porph)(L)] structures with 1-MeIm or 1-EtIm ligands. The three structures have the same metal out of plane displacement, but different axial bond lengths. Examination of the first two structures suggests that the larger tilt angle of 10.9° corresponds to the longer Mn—N<sub>im</sub> distance (2.192(2) Å), while the smaller tilt angle of 5.2° corresponds to the shorter Mn—N<sub>im</sub> distance (2.168(5) Å). The off-axis tilt causes nonbonded interactions between the five-membered imidazole ring and the porphyrin plane. A large tilt weakens the σ+π bonding between the ligand and the metal atom. Raman studies of high spin deoxyhemoglobins have revealed that an increasing tilt of histidine ligand results in an increase in repulsive forces between the imidazole carbon and the heme plane. This increase in repulsive force weakens the Fe—N<sub>HIS</sub> bond, thereby lowering the frequency of the Fe—N<sub>HIS</sub> stretching mode.<sup>27</sup> Thus the observed structural correlation between ligand tilting angles and axial bond distances is consistent with the reports.

**Scheme 1** Formal Diagrams of Structures of Five-Coordinate [M(TpivPP)(2-MeHIm)] (M = Mn, Fe and Co).<sup>a</sup>

<sup>a</sup> Scheme is edge-on view of the porphyrin plane and ligands with the key parameters (distances in Å, angles in degrees) of  $\Delta_{24}$ ,  $\tau$ ,  $(M-N_p)_{av}$ ,  $M-N_{im}$ ,  $M-N_{im}-C_{im}(2)$  and  $M-N_{im}-C_{im}(4)$ . The structural parameters of [M(TpivPP)(2-MeHIm)] (M = Fe and Co) were obtained from ref.22,21.

**Scheme 2.** Formal Diagrams of Structures of Five-Coordinate [Mn(Porph)(R-Im)] (R-Im = 1-MeIm or 1-EtIm).<sup>a</sup>

<sup>a</sup> Scheme is edge-on view of the porphyrin plane and ligands with the key parameters (distances in Å, angles in degrees) of  $\Delta_{24}$ ,  $\tau$ ,  $(Mn-N_p)_{av}$ ,  $Mn-N_{im}$ ,  $Mn-N_{im}-C_{im}(4)$ . The structural parameters of [Mn(TPP)(1-MeIm)] were obtained from ref.13.

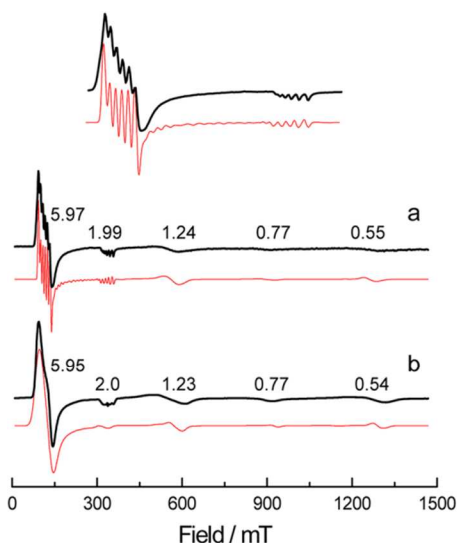


**Figure 5.** X-band EPR spectra of [Mn(TpivPP)(2-MeHIm)] at 90 K (black lines) and its simulation (red lines). a.  $CH_2Cl_2$  solution, in order to clearly see the hyperfine splitting, the amplified portion is shown at the top of the figure. b. ground microcrystalline. EPR simulation conditions, see Electronic Supplementary Information.

### EPR spectroscopy

High field EPR studies have been performed on [Mn(TpivPP)(1-MeIm)] (powder) and [Mn(TpivPP)(2-MeHIm)] (powder and solution) at 90 K. The spectra of [Mn(TpivPP)(2-MeHIm)] and its simulation are given in Figure 5 and those of [Mn(TpivPP)(1-MeIm)] will be found in Figure S8. The two complexes present similar EPR spectra. Both give five resonances at similar positions in the experimental field. The two spectra of [Mn(TpivPP)(2-MeHIm)] in solid and solution states are also consonant. The first systematic EPR study on Mn(II) heme complexes was reported at 1970.<sup>28</sup> The X-band EPR at 77 K gave four resonances at the positions of 5.9, 2.0, 1.21 and 0.77. Later, [Mn(TPP)(Py)] (Py = pyridine), was studied at 77 K and two resonances were recognized at 5.96 and 2.00.<sup>29</sup> Our experimental results are consistent with these reports showing characteristic resonances of high spin manganese porphyrinates at  $\sim 5.9$  ( $g_{\perp}$ ) and  $\sim 2.0$  ( $g_{\parallel}$ ). In addition, we are able to observe the other three resonances including the fifth resonance at  $\sim 0.55$ . The fifth position at  $\sim 0.55$  would correspond to the transition,  $M_s = -1/2 \leftrightarrow -3/2$ , with the magnetic field parallel to the  $z$  axis, which has not been observed at temperatures higher than 5 K.<sup>30</sup> The information is summarized in Table 3.

The high spin Mn(II) ion ( $3d^5$ ) is characterized by an electronic spin  $S = 5/2$  and a nuclear spin  $I = 5/2$ . Its electronic

properties can be described by the following Hamiltonian:

$$H = \beta B g S + IAS + D[S_z^2 - \frac{1}{3}S(S+1)] + E(S_x^2 - S_y^2) \quad (1)$$

The first two terms stand for the Zeeman and electron nuclear hyperfine interactions respectively; while the last two terms define the zfs (zero field splitting), with  $D$  and  $E$  denoting the magnitude of axial and rhombic components, respectively.<sup>31</sup>

All species in Table 3 have two characteristic signals at  $g_{\perp} \sim 5.9$  and  $g_{\parallel} \sim 2.0$ . The samples in the glass state give resolved hyperfine splitting from the manganese nucleus ( $I = 5/2$ ). These observations suggest that the strong tetragonal field results in  $D \gtrsim g\beta H$  and transitions within the lowest lying Kramers doublet ( $|\pm 1/2\rangle$ ) have  $g$  values near 6 ( $g_{\perp}$ ) and 2 ( $g_{\parallel}$ ).<sup>32</sup> This situation is analogous to that of the high-spin Fe(III) porphyrin complexes. However, the magnitude of the zfs in the Mn(II) species is an order of magnitude less than in the Fe(III) complexes.<sup>28,33</sup> We determined the spin Hamiltonian parameters by using a full-matrix diagonalization procedure of eq. (1) that simulates the EPR data. The resulting  $D$ ,  $E$  and their ratio  $E/D$  ( $\lambda$ ), and hyperfine coupling constants  $A$  are given in Table 3. It is seen that Mn(TpivPP)(1-MeIm) and [Mn(TpivPP)(2-MeHIm)] show consistent parameters values which are comparable to previous results. The  $D$  values

are larger than the reported values  $\sim 0.55 \text{ cm}^{-1}$  of Mn(II) protoporphyrin IX, and at the upper extreme of the order of 0.5 to  $0.7 \text{ cm}^{-1}$ .<sup>28</sup> The  $\lambda$  in these Mn(II) heme complexes is small and is  $\leq 0.01$ .<sup>34</sup> The simulated hyperfine coupling constants  $A$  are also comparable to that of [Mn(TPP)(Py)] and manganese (II) protoporphyrin IX derivatives ( $A_{\perp} = 0.0073$  and  $A_{\parallel} = 0.011 \text{ cm}^{-1}$ ), and is smaller than the typical value of  $8.88 \times 10^{-3} \text{ cm}^{-1}$  (-95 Gauss) for an octahedral coordinated Mn(II) ion.<sup>33</sup>

## Conclusions

Three five-coordinate imidazole ligated manganese (II) "picket fence" porphyrinates have been prepared and characterized by single-crystal X-ray, EPR and UV-vis spectroscopies. The new structures show typical characteristics of high-spin manganese(II) porphyrin complexes which include large metal displacements, long Mn—N<sub>p</sub> bond distances and domed porphyrin cores. EPR measurements observed five resonances including characteristic signals at  $\sim 5.9$  and  $\sim 2.0$ . The simulations gave reasonable zfs parameters for  $D$ ,  $E$  and hyperfine coupling constants  $A$ , which suggests strong tetragonal field and the transitions within the lowest lying Kramers doublet ( $|\pm 1/2\rangle$ ).

Table 3. EPR Parameters for High Spin Five-Coordinate Manganese(II) Porphyrin Complexes

complex	$g_1$	$g_2$	$g_3$	$g_4$	$g_5$	T <sup>a</sup>	phase	$D^b$	$E^c$	$\lambda^d$	$A_{\perp}^e$	$A_{\parallel}^e$	ref.
[Mn(TpivPP)(1-MeIm)] <sup>e</sup>	5.94	1.98	1.24	0.78	0.55	90	powder	0.68	3.38	5	7.0	9.0	tw
[Mn(TpivPP)(2-MeHIm)] <sup>e</sup>	5.95	2.0	1.23	0.77	0.54	90	powder	0.69	3.47	5	7.3	8.7	tw
	5.97	1.99	1.24	0.77	0.55	90	solution	0.67	3.37	5	7.3	8.7	tw
[Mn(TPP)(Py)]	5.96	2.00				77	solution	> 0.3			6.9		29
Mn-CCP <sup>f</sup>	5.9	2.0	1.21	0.77		77	solution	0.56		$\sim 20$	7.3	11	28
Mn-Hb <sup>f</sup>	5.9	2.0				77	solution	0.54		10			28
Mn-HRP <sup>f</sup>	5.9	2.0				77	solution	0.5		< 2			28
Mn-Mb <sup>f</sup>	5.9	2.0				77	solution	0.56		< 5			28

<sup>a</sup> Values in K. <sup>b</sup> Values in  $\text{cm}^{-1}$ . <sup>c</sup> Values in  $\times 10^{-3} \text{ cm}^{-1}$ . <sup>d</sup>  $\times 10^{-3}$ . <sup>e</sup> These  $g$  values were obtained from the X-band spectra at 90 K;  $D$ ,  $E$  and  $A$  were estimated from EasySpin simulation, see ESI. <sup>f</sup>  $D$  was estimated from positions of X- and K-band transitions at 77 K;  $\lambda$  was estimated from the number and line shape of hyperfine lines in the X-band transitions at  $g_{\perp} = 5.9$ ; CCP, Hb, HRP, Mb see ref.35.

## Acknowledgements

We thank the CAS Hundred Talent Program and National Natural Science Foundation of China (Grant no. 21371167) to J.L.

## Notes and references

<sup>a</sup> Research Institute of Applied Chemistry, Shanxi University, Taiyuan, 030006, China.

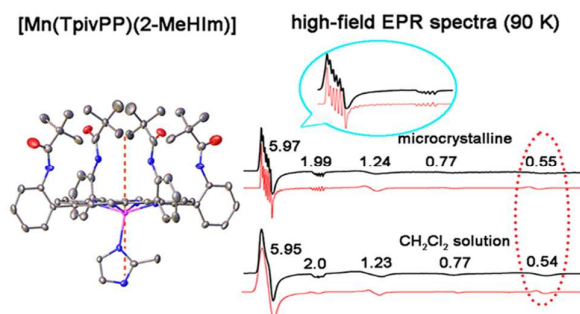
<sup>b</sup> College of Materials Science and Opto-electronic Technology, University of Chinese Academy of Sciences, YanQi Lake, HuaiRou District, Beijing, 101408, China

<sup>c</sup> Technical Institute of Physics and Chemistry, 29 ZhongGuanCun East Road, Haidian District, Beijing, 100190, China.

Electronic Supplementary Information (ESI) available: [UV-vis spectra; figures with ORTEP diagrams; EPR spectra of [Mn(TpivPP)(1-Melm)] and its simulation; the simulation conditions.]. See DOI: 10.1039/b000000x/

- E. Antonini and M. Brunori, *Hemoglobin and Myoglobin in their Reactions with Ligands*, North-Holland, Amsterdam, 1971.
- (a) M. F. Perutz, *Nature*, 1970, **228**, 726; (b) M. F. Perutz, *Nature*, 1972, **237**, 495.
- (a) M. Paoli, G. Dodson, R. C. Liddington and A. J. Wilkinson, *J. Mol. Biol.*, 1997, **271**, 161; (b) J. Baldwin and C. Chothia, *J. Mol. Biol.*, 1979, **129**, 175.
- S. S. Stavrov, *Biophys. J.*, 1993, **65**, 1942.
- (a) W. R. Scheidt and C. A. Reed, *Chem. Rev.*, 1981, **81**, 543; (b) W. R. Scheidt, in *The Porphyrin Handbook*, eds. K. M. Kadish, K. M. Smith and R. Guilard, Academic Press, San Diego, 2000, vol. 3, pp. 49.
- G. B. Jameson, F. S. Molinaro, J. A. Ibers, J. P. Collman, J. I. Brauman, E. Rose and K. S. Suslick, *J. Am. Chem. Soc.*, 1980, **102**, 3224.
- (a) M. K. Ellison, C. E. Schulz and W. R. Scheidt, *Inorg. Chem.*, 2002, **41**, 2173; (b) C. Hu, A. Roth, M. K. Ellison, J. An, C. M. Ellis, C. E. Schulz and W. R. Scheidt, *J. Am. Chem. Soc.*, 2005, **127**, 5675; (c) C. Hu, J. An, B. C. Noll, C. E. Schulz and W. R. Scheidt, *Inorg. Chem.*, 2006, **45**, 4177; (d) C. Hu, B. C. Noll, C. E. Schulz and W. R. Scheidt, *Inorg. Chem.*, 2010, **49**, 10984.
- J. P. Collman and C. A. Reed, *J. Am. Chem. Soc.*, 1973, **95**, 2048.
- (a) M. S. Liao and S. Scheiner, *J. Chem. Phys.*, 2002, **116**, 3635; (b) J. M. Ugalde, B. Dunietz, A. Dreuw, M. Head-Gordon and R. J. Boyd, *J. Phys. Chem. A*, 2004, **108**, 4653; (c) C. Rovira, K. Kunc, J. Hutter, P. Ballone and M. Parrinello, *J. Phys. Chem. A*, 1997, **101**, 8914.
- W. R. Scheidt, D. K. Geiger, Y. J. Lee, C. A. Reed and G. Lang, *J. Am. Chem. Soc.*, 1985, **107**, 5693.
- A. Ikezaki, M. Takahashi and M. Nakamura, *Angew. Chem. Int. Edit.*, 2009, **48**, 6300.
- (a) C. Bull, R. G. Fisher and B. M. Hoffman, *Biochem. Biophys. Res. Commun.*, 1974, **59**, 140; (b) Q. H. Gibson, B. M. Hoffman, R. H. Crepeau, S. J. Edelstein and C. Bull, *Biochem. Biophys. Res. Commun.*, 1974, **59**, 146; (c) B. M. Hoffman, Q. H. Gibson, C. Bull, R. H. Crepeau, S. J. Edelstein, R. G. Fisher and M. J. McDonald, *Ann. Ny. Acad. Sci.*, 1975, **244**, 174.
- J. F. Kirner, C. A. Reed and W. R. Scheidt, *J. Am. Chem. Soc.*, 1977, **99**, 2557.
- J. P. Collman, R. R. Gagne, C. A. Reed, T. R. Halbert, G. Lang and W. T. Robinson, *J. Am. Chem. Soc.*, 1975, **97**, 1427.
- G. M. Sheldrick, *Acta Crystallogr., Sect. A*, 2008, **64**, 112.
- $R_1 = \sum \|F_o\| - |F_c| / \sum |F_o|$  and  $wR_2 = \{ \sum [w(F_o^2 - F_c^2)^2] / \sum [wF_o^4] \}^{1/2}$ . The conventional  $R$ -factors  $R_1$  are based on  $F$ , with  $F$  set to zero for negative  $F^2$ . The criterion of  $F^2 > 2\sigma(F^2)$  was used only for calculating  $R_1$ .  $R$ -factors based on  $F^2$  ( $wR_2$ ) are statistically about twice as large as those based on  $F$ , and  $R$ -factors based on all data will be even larger.
- G. M. Sheldrick, *Program for Empirical Absorption Correction of Area Detector Data*, Universität Göttingen, Germany, 1996.
- CrysAlisPro, Oxfordshire, U.K., Oxford Diffraction Ltd edn., 2010.
- EasySpin is a numerical EPR toolbox for MATLAB available at [www.esr.ethz.ch](http://www.esr.ethz.ch). (accessed Jan. 2014).
- C. A. Reed, J. K. Kouba, C. J. Grimes and S. K. Cheung, *Inorg. Chem.*, 1978, **17**, 2666.
- J. Li, B. C. Noll, A. G. Oliver, G. Ferraudi, A. G. Lappin and W. R. Scheidt, *Inorg. Chem.*, 2010, **49**, 2398.
- J. Li, B. C. Noll, A. G. Oliver, C. E. Schulz and W. R. Scheidt, *J. Am. Chem. Soc.*, 2013, **135**, 15627.
- J. Li, B. C. Noll, A. G. Oliver and W. R. Scheidt, *J. Am. Chem. Soc.*, 2012, **134**, 10595.
- (a) H. C. Stynes and J. A. Ibers, *J. Am. Chem. Soc.*, 1972, **94**, 1559; (b) D. V. Stynes, H. C. Stynes, B. R. James and J. A. Ibers, *J. Am. Chem. Soc.*, 1973, **95**, 1796.
- W. R. Scheidt and Y. Lee, in *Metal Complexes with Tetrapyrrole Ligands I*, ed. J. Buchler, Springer Berlin Heidelberg, 1987, vol. 64, pp. 1.
- R. Shannon, *Acta Crystallogr., Sect. A*, 1976, **32**, 751.
- (a) J. Friedman, D. Rousseau, M. Ondrias and R. Stepnoski, *Science*, 1982, **218**, 1244; (b) J. M. Friedman, T. W. Scott, R. A. Stepnoski, M. Ikeda-Saito and T. Yonetani, *J. Biol. Chem.*, 1983, **258**, 10564.
- T. Yonetani, H. R. Drott, J. S. Leigh, G. H. Reed, M. R. Waterman and T. Asakura, *J. Biol. Chem.*, 1970, **245**, 2998.
- B. M. Hoffman, C. J. Weschler and F. Basolo, *J. Am. Chem. Soc.*, 1976, **98**, 5473.
- H. Hori, M. Ikeda-Saito, G. H. Reed and T. Yonetani, *J. Magn. Reson.*, 1984, **58**, 177.
- A. Abragam and B. Bleaney, *Electron Paramagnetic Resonance of Transition Ions*, Dover Publications, New York, 1986.
- G. W. Brudvig, in *Advanced EPR*, ed. A. J. Hoff, Elsevier, Amsterdam, 1989, pp. 839.
- G. Reed and G. Markham, in *Biological Magnetic Resonance*, eds. L. Berliner and J. Reuben, Springer US, 1984, pp. 73.
- R. D. Dowsing and J. F. Gibson, *J. Chem. Phys.*, 1969, **50**, 294.
- CCP, cytochrome c peroxidase; Hb, hemoglobin; HRP, horseradish peroxidase; Mb, myoglobin.

- a graphical and textual abstract for the contents pages



The X-ray structural investigation rationalized the variable axial ligand distances. EPR revealed the unprecedented, fifth resonance position at  $\sim 0.55$ , and the simulations gave reasonable zero field splitting parameters.